Dalton Transactions

Accepted Manuscript

ROYAL SOCIETY OF CHEMISTRY

www.rsc.org/dalton

Journal Name

RSCPublishing

ARTICLE

Synthesis and Spectroscopic Properties of Yb^{3+} and Tb^{3+} Co-doped $GdBO_3$ Materials Showing Down- and Up-conversion Luminescence

Tomasz Grzyb*, Konrad Kubasiewicz, Agata Szczeszak and Stefan Lis

Cite this: DOI: 10.1039/x0xx00000x

Received ooth January 2012,
Accepted ooth January 2012

DOI: 10.1039/x0xx00000x

www.rsc.org/

Gadolinium orthoborates doped with Yb^{3+} and Tb^{3+} ions were synthesised by the sol-gel Pechini method. Materials annealed at 900 °C were composed of the monoclinic $GdBO_3$ phase with micrometre-sized crystals. Structural properties of the products were analysed by X-ray diffraction (XRD) and transmission electron microscopy (TEM). Composition of the prepared materials was determined with inductively coupled plasma optical emission spectroscopy (ICP-OES). The materials showed intense ultraviolet (UV) or near infrared (NIR) excited green emission, which resulted from down- or up-conversion processes taking place in their structure. Spectroscopic properties were investigated on the basis of measured excitation and emission spectra. Also, luminescence decays showing a short rise of emission in time after NIR excitation were measured. The dependence of integral up-conversion intensity on the energy of the pumping laser was measured. The results indicated a two-photon process based on cooperative energy transfer (CET). The analysis of synthesised series of samples allowed to indicate those with the best emission under a UV or NIR excitation source.

1. Introduction

For many years much attention has been paid to inorganic nanophosphors, including rare earth orthoborates, e.g. $REBO_3$ (RE = Y, La, Gd), due to their efficient visible emission whose colour depends on the dopant ion, e.g. red for Eu^{3+} or green when Tb^{3+} is used.[1–4] Luminescence of $REBO_3$-based materials can be activated by radiation from vacuum ultraviolet (VUV) to ultraviolet (UV).[5,6] Additionally, their chemical and thermal stability allows to employ such compounds in a variety of applications, such as colour plasma display panels or Hg-free fluorescent lamps.

Currently, a number of studies is being carried out to find ideal materials that could be used in medicine and biology for fluorescence imaging. Increasingly more often, up-converting nanoparticles (UCNPs) doped with lanthanide ions, Ln^{3+}, are being considered for bioimaging, biolabelling or drug delivery.[7,8] Such a type of nanosystems is highly promising due to their intense visible emission based on the anti-Stokes up-conversion process, which is especially efficient in lanthanide-doped inorganic materials.[9] The most often studied systems are based on fluorides as host materials and the following pairs of ions: Yb^{3+}/Er^{3+}, Yb^{3+}/Tm^{3+} or Yb^{3+}/Ho^{3+}.[2,10,11] However, in some cases also efficient emission from other, less studied pairs can be obtained, e.g. Yb^{3+}/Eu^{3+} or Yb^{3+}/Tb^{3+}.[12–15]

Dual-mode luminescence, based on down- and up-conversion is an interesting phenomenon, which can be used in the designing of materials for special applications. Nanoparticles showing UV or NIR excited luminescence can be applied in multiplexed and highly sensitive bioassays.[16] Also advanced security markers, can be based on the dual-mode emission what gives a new opportunities for anti-counterfeiting aplications.[17]

Generally, the mechanism of up-conversion luminescence consists in the conversion of near infrared (NIR) or infrared (IR) low-energy radiation to high-energy UV or visible (Vis) light.[9] In the former group of dopant pairs, visible emission is possible due to ground- or excited-state absorption (GSA or ESA, respectively) and energy transfer up-conversion (ETU). However, for Yb^{3+}/Tb^{3+} and Yb^{3+}/Eu^{3+} systems, the mechanism of anti-Stokes emission involves cooperative energy transfer (CET) from Yb^{3+} to Tb^{3+} or Eu^{3+} ions.[15,18–19] Most often, low phonon energy of the matrix, e.g. fluorides promote efficient emission by diminution of multiphonon quenching of an

emitting ion.[20] However, the CET between Yb^{3+} and Tb^{3+} ions is possible in host matrices, such as $REBO_3$, which exhibit higher phonon energy in comparison, for example, to fluorides (350 cm^{-1} and ~1000 cm^{-1}, respectively).[20,21] Otherwise, non-radiative transfer of energy takes place and Yb^{3+} quenches Tb^{3+} emission by a phonon-assisted energy transfer.[22]

Many attempts have been made to determine and systematise the crystal structure of $REBO_3$ compounds. Levin et al. began with a division into three fundamental crystal structures of $REBO_3$, aragonite, calcite and vaterite, which are analogous to the crystalline forms of $CaCO_3$. The crystal structure of $REBO_3$ depends on the ionic radius of the rare earth ion. These compounds crystallise in orthorhombic, trigonal or hexagonal systems, respectively.[23] Then several papers discussed different types of crystal structure, space groups and point symmetry sites.[24–31] More recently, $ErBO_3$ nanocrystals were synthesised and their crystal structure was confirmed as a monoclinic pseudowollastonite-type structure, space group $C2/c$.[32] Most recently, we published two new structures, i.e. monoclinic and triclinic ones, determined for the $GdBO_3$ nanopowders and synthesised by the sol-gel Pechini and hydrothermal method, respectively.[6,33]

According to our knowledge, no articles have been published describing down- and up-conversion in gadolinium orthoborate based on cooperative energy transfer (CET) between Yb^{3+} and Tb^{3+} dopant ions. This type of down and up-conversion mechanism was investigated in our earlier work in $GdPO_4$:Yb^{3+},Tb^{3+} and $LaPO_4$:Yb^{3+},Tb^{3+} nanocrystals.[14,15] In that paper, the modified sol-gel Pechini method of synthesis was used to obtain monoclinic $GdBO_3$:Yb^{3+},Tb^{3+} materials. The Pechini method allows to prepare powders with proper homogeneity, crystallinity and relatively small particle size without using advanced and expensive equipment or complicated procedures. A detailed structural and photophysical characterisation of the synthesised materials was made. The luminescence properties of up-converting $GdBO_3$:Yb^{3+},Tb^{3+} powders were carefully studied.

2. Experimental

2.1. Synthesis

$GdBO_3$:Yb^{3+},Tb^{3+} nanopowders were synthesised by the modified sol-gel Pechini method. Appropriate oxides of rare earth elements: Gd_2O_3, Yb_2O_3, Tb_4O_7 (99.99%; Stanford Materials, United States), were dissolved in nitric acid HNO_3 (ultra-pure; POCh S.A., Poland) in order to obtain nitrates $RE(NO_3)_3$. An excess amount of acid was removed by evaporating the solutions several times. In the first step, citric acid monohydrate (p.a. grade; CHEMPUR, Poland) and ethylene glycol (p.a. grade; CHEMPUR, Poland) were mixed together in deionised water with stoichiometric amounts of $RE(NO_3)_3$ solutions. An excess of citric acid (12 g per 1 g of product) and ethylene glycol (1 mL per 1 g of product) was added. Then an aqueous solution of orthoboric acid H_3BO_3 (p.a.; POCh S.A., Poland) was poured into the solution with 100% excess to the stoichiometric amount. The homogeneous solution was dried at 80 °C for 24 h to remove water and to provide a co-polymerisation reaction and gel formation. Finally, the dark resin was annealed at 900 °C for 3 h and white powders were obtained.

2.2. Apparatus

X-ray diffraction (XRD) patterns were measured using a Bruker AXS D8 Advance diffractometer in Bragg-Brentano geometry, with Cu $K_{\alpha 1}$ radiation (λ = 1.541874 Å) in the 2θ range from 6° to 60°. The reference data were taken from our previous paper, in which we revised the structural properties of $GdBO_3$ synthesised by the sol-gel Pechini method.[6] Transmission electron microscopy (TEM) images were collected on a FEI Tecnai G2 20 X-TWIN transmission electron microscope, which used an accelerating voltage of 200 kV. The composition of the prepared materials was determined with a Varian ICP-OES VISTA-MPX inductively coupled plasma optical emission spectrometer. The composition of the samples was similar to the theoretical composition, e.g. the analysed dopant concentrations in the sample $GdBO_3$:15%Yb^{3+},15%Tb^{3+} were 17%Yb^{3+} and 16% Tb^{3+}, or in sample $GdBO_3$:10%Yb^{3+},30%Tb^{3+} they were 10% Yb^{3+} and 27% Tb^{3+}.

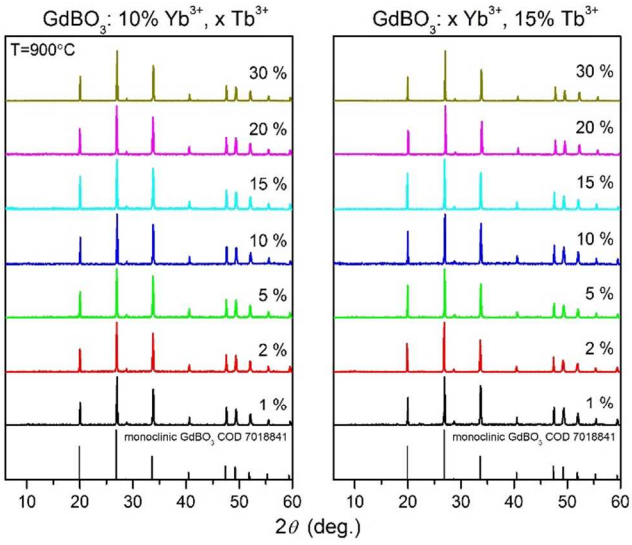

Fig 1 XRD diffractograms of $GdBO_3$ doped with Yb^{3+} and Tb^{3+} ions after annealing at 900 °C for 2 h.

The excitation spectra of the samples were measured on a Hitachi F-7000 fluorescence spectrophotometer equipped with a 150 W xenon lamp. Excitation spectra were corrected for instrumental response. A QuantaMasterTM 40 spectrophotometer equipped with an Opolette 355LD UVDM tunable laser as the excitation source and a Hamamatsu R928 photomultiplier as a detector were used for the emission and luminescence decay measurements. All measurements were done at room temperature.

3. Results and discussion

3.1. Structure and morphology

The synthesised materials crystallised as monoclinic crystals with the space group of *C*2/*c*. Experimental XRD patterns presented in Fig. 1 fit well with the theoretical diffractogram taken from the Crystallographic Open Database and from our previous results.[6] The dopants were neutral for the phase composition and no impurities of other compounds were found. The previously described method and appropriately selected amount of H_3BO_3 in the gel precursor were responsible for high purity of the obtained samples.[6] A smaller amount of this reagent caused the formation of an extra phase of triclinic $GdBO_3$. The excess of H_3BO_3 was employed to equalise evaporation loss. Well-defined XRD peaks and their narrow shape confirmed high crystallinity of the products. Small full-width at half maximum (FWHM) indicates an average size of individual crystals above 100 nm.

There are two types of Gd^{3+} sites in the crystallographic structure of $GdBO_3$. Both are 8-coordinated by O^{2-} anions. The symmetries of these sites are: C_i and C_1 with a ratio of 1:2.[34]

TEM images (Fig. 2) of the synthesised materials show a plate-like shape of the crystals with quite an irregular structure caused by annealing conditions. The crystals sintered and formed aggregates. However, their sizes are similar and in the range of 400-600 nm.

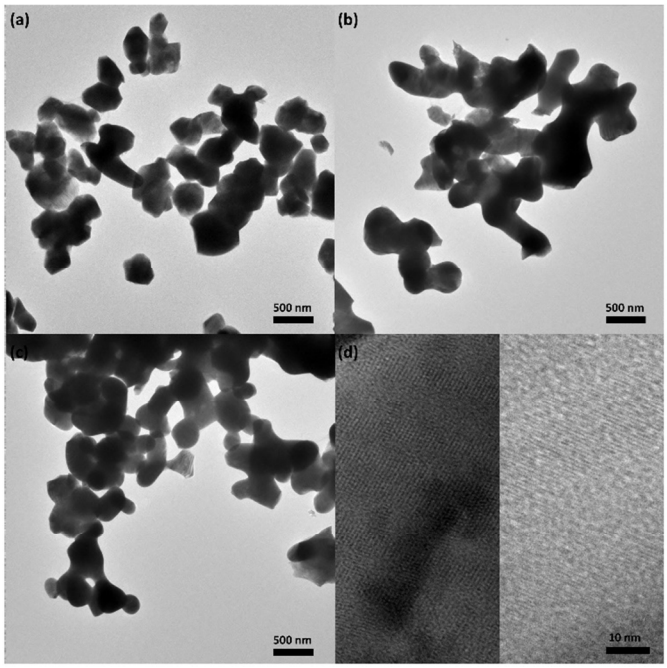

Fig. 2 TEM images of $GdBO_3$ annealed at 900 °C for 2 h: (a) pure host material, (b) $GdBO_3$ doped with 10% Yb^{3+} and 15% Tb^{3+} ions and (c,d) doped with 10% Yb^{3+} and 20% Tb^{3+}.

3.2. Spectroscopic properties

The $GdBO_3$:Yb^{3+},Tb^{3+} material can be excited by UV or by NIR radiation as a result of *f-d* and *f-f* electronic transitions within Tb^{3+} ions and as a consequence of Yb^{3+} absorption and energy transfer between dopant ions.[14] Luminescence excitation spectra were measured in the range of 200–400 nm and are presented in Fig. 3. Broad excitation peaks at shorter wavelengths and a series of narrower peaks at lower energies can be observed. Broad excitation bands with maxima at around 230 nm in each sample are connected with the $4f^8 \rightarrow 4f^7 5d^1$ transition of Tb^{3+} ions. The bands appearing above 250 nm originate from *f–f* electronic transitions of Gd^{3+} and Tb^{3+} ions. Excitation of the 4*f* electrons of the Tb^{3+} ion results in their promotion to the excited 5*d* shell. Hence, excited states with two configurations, i.e. the high-spin ^9D_J state and the ^7D_J low-spin state, are formed.[35] The ^9D_J states have lower energy than the ^7D_J states (Hund's rule), but only the spin-allowed $^7F_J \rightarrow {}^7D_J$ transitions can be observed and are connected with the excitation band with a maximum at around 230 nm.[36] Spin-forbidden $^7F_J \rightarrow {}^9D_J$ transitions were not observed in our samples.

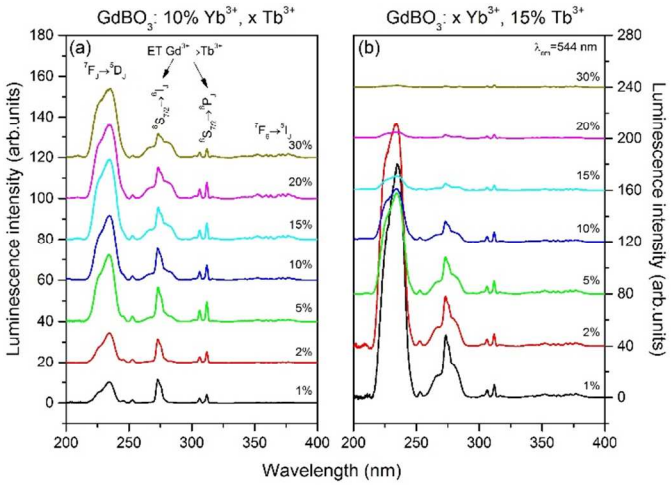

Fig. 3 Excitation spectra of $GdBO_3$:Yb^{3+},Tb^{3+} materials (λ_{em} = 544 nm); dependence on Tb^{3+} (a) and Yb^{3+} (b) concentrations.

The two groups of excitation bands that appeared in the range of 250–325 nm are connected with $^8S_{7/2} \rightarrow {}^6I_J$ and $^8S_{7/2} \rightarrow {}^6P_J$ transitions of Gd^{3+} ions and confirm a direct energy transfer between Gd^{3+} and Tb^{3+} ions. The small peaks above 350 nm are the excitation bands of Tb^{3+} ions. The relatively small intensity shows how ineffective direct excitation into the parity-forbidden *f-f* electronic transitions of Tb^{3+} ions is.

The excitation spectra presented as depending on the Yb^{3+} concentration (see Fig. 3b) show that the intensity of the $^7F_J \rightarrow {}^7D_J$ transition band is sensitive to the concentration of Yb^{3+} ions and that increasing the concentration of these ions reduces the intensity of the excitation peak. An explanation for this phenomenon is the charge transfer between the Tb^{3+} and Yb^{3+} ions occurring in the prepared materials after UV irradiation.[37,38] The formation of a charge transfer state (CTS) is the result of the tendency of Tb^{3+} ions to be oxidised and the

easiness of Yb^{3+} ion reduction. Under UV light the Tb^{3+} ions are excited into the $4f^7 5d^1$ state, from which energy is transferred to the Yb^{3+} ions with the formation of the intermediate, Tb^{4+}-Yb^{2+} CTS.[37] Next, Yb^{3+} ions are radiative deexcitated with emission of NIR light. This process could be important for applications requiring down-conversion of UV light, and it is known to be highly efficient.[39]

Green luminescence of the $GdBO_3$:Yb^{3+},Tb^{3+} materials shows a dependence on the Tb^{3+} ion concentration. The ions are known from cross relaxation (CR) of the higher excited states as well as relatively high concentration quenching.[40] Fig. 4 shows the luminescence spectra of Yb^{3+} and Tb^{3+} co-doped $GdBO_3$ materials after excitation with UV light (235 nm). The presented spectra demonstrate characteristic luminescence bands connected with *f–f* electronic transitions of Tb^{3+} ions. Emissions from higher, $^5G_6$ and $^5D_3$, levels were not observed in all the samples due to CR processes connected with Tb^{3+} ions.[41,42] The insets presented in Fig. 4 show the integral luminescence

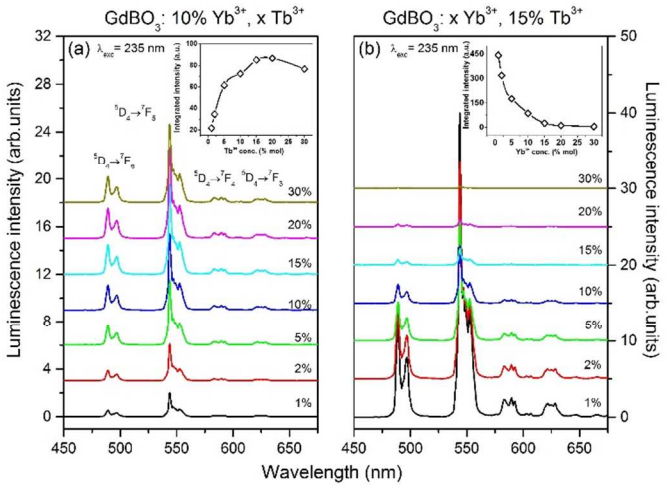

Fig. 4 Emission spectra of $GdBO_3$:Yb^{3+},Tb^{3+} materials (λ_{ex} = 235 nm); dependence on Tb^{3+} (a) and Yb^{3+} (b) concentrations and as insets: dependence of integral intensity on Tb^{3+} (a) and Yb^{3+} (b) concentrations.

intensity of Tb^{3+} ions depending on the concentration of (a) Tb^{3+} or (b) Yb^{3+} ions. The highest luminescence intensity was observed for samples doped with 15% of Tb^{3+} ions. Concentrations of Tb^{3+} ions higher than 20% cause quenching of green luminescence. The addition of Yb^{3+} ions into $GdBO_3$:Tb^{3+} resulted in a reduction of Tb^{3+},green emission. The Yb^{3+} ions strongly quench Tb^{3+} ion emission. The energy of the Tb^{3+} ion can be cooperatively transferred from the Tb^{3+} ion in its $^5D_4$ excited state to two Yb^{3+} ions.[14,37] This effect can be observed in the luminescence intensity as well as in the shortening of luminescence lifetimes in the whole range of Yb^{3+} concentrations (see Fig. 7).

Up-conversion of $GdBO_3$:Yb^{3+},Tb^{3+} materials under excitation with a 973 nm laser are presented in Fig. 5. The spectra characteristics are almost identical with those obtained under UV excitation, which arises from the properties of Tb^{3+} ions; only the intensities were alternated. Maximum up-conversion emission should be expected for samples doped with 20% of Tb^{3+} and 5% of Yb^{3+} ions when the insets presented in Fig. 5 are taken into account. Integral luminescence intensity depended on the concentration of Tb^{3+} or Yb^{3+} ions, which resulted from the cross relaxation and energy quenching properties of Yb^{3+} ions.

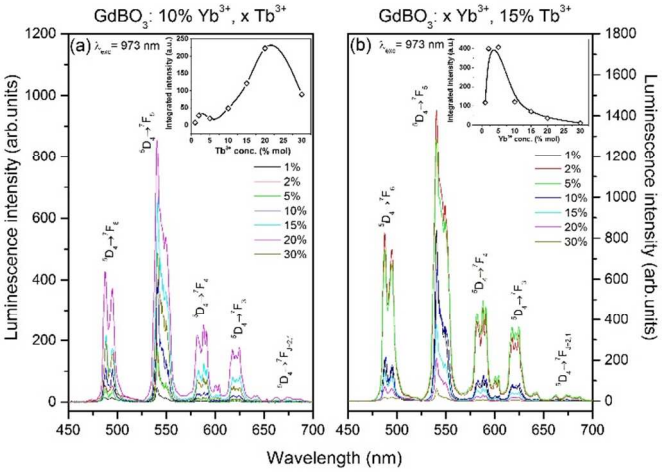

Fig. 5 Dependence of up-conversion luminescence spectra of $GdBO_3$:Yb^{3+},Tb^{3+} materials on concentrations of Tb^{3+} (a) and Yb^{3+} (b); insets: dependence of integral intensity on concentrations of Tb^{3+} (a) and Yb^{3+} (b).

As should be supposed, considering CET as the main mechanism of observed emission, a relatively large part of Gd^{3+} ions in the host material must be replaced, especially by the acceptor Tb^{3+} ions.[43]

Figs 6a-d present the luminescence decays of Tb^{3+} and Yb^{3+} ions in all samples measured using UV (235 nm) and NIR laser light (973 nm). These are strongly dependent on the concentrations of dopant ions. They have a non-exponential character and, additionally, those obtained after excitation with 973 nm present a short rise of luminescence after the excitation pulse. This observation is a direct result of the energy transfer between Yb^{3+} and Tb^{3+} ions. An increasing concentration of Yb^{3+} ions does not significantly change the shape of the collected decays; but when the Tb^{3+} ion concentration increases, the character of the observed curve changes, which suggests that Tb^{3+}-Tb^{3+} interaction appeared.

The recorded decays were used to calculate luminescence lifetimes (see Fig. 7), assuming that they can be approximated by

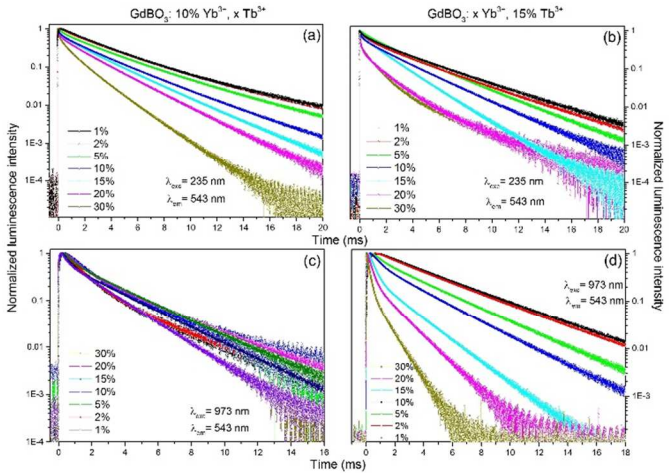

Fig. 6 Luminescence decays of $GdBO_3$:Yb^{3+},Tb^{3+} materials during observation of Tb^{3+} emission under λ_{ex} = 235 nm (a, b) or λ_{ex} = 973 nm (c, d), which are dependent on Tb^{3+} (a, c) or Yb^{3+} (b, d) concentrations.

using an exponential function. The following single exponential function was used for the Tb^{3+} lifetime calculations after UV excitation:

$$I = I_0 \cdot e^{-\frac{t}{\tau}} \quad (1)$$

where I represents intensity at any time, I_0 is the intensity at t = 0 and τ is the luminescence lifetime.

Because decays obtained as the result of up-conversion present a rise time, the calculations of luminescence lifetimes as well as rise times were done using the following equation:

$$I = [I_0 + I_1(1 - e^{-\frac{t}{\tau_r}})]e^{-\frac{t}{\tau_d}} \quad (2)$$

where I_0 is the initial luminescence intensity at time t = 0, I_1 is the intensity added by energy transfer, and τ_r and τ_d are the rise and decay times, respectively. The calculated luminescence lifetimes and rise times are compared in Fig. 7.

The calculated values of lifetimes show a dependence on the dopant concentrations and became shorter with increasing amounts of Tb^{3+} or Yb^{3+} ions in the $GdBO_3$ host for the 235 nm excitation wavelength that was used. The up-conversion luminescence lifetime values initially increase with the increasing amount of Gd^{3+} ions in the host. Higher than 15% of Tb^{3+}-doped samples are quenched by cross relaxation processes, therefore the lifetime becomes shorter. The effects of an increasing concentration of Yb^{3+} ions on the emission of Tb^{3+} ions shows the effectiveness of these ions' quenching properties for Tb^{3+} luminescence. The calculated values of the luminescent lifetimes of Tb^{3+} ions are similar to those in the literature and are in the range of 0.3–3.9 ms.[14,44] The rise times presented in Figs 7c and d are in the range of 6–270 μs and become shorter with increasing concentrations of luminescent Tb^{3+} or sensitising Yb^{3+} ions. The reason for this observation is that the average distance between the donor and acceptor ions is smaller and

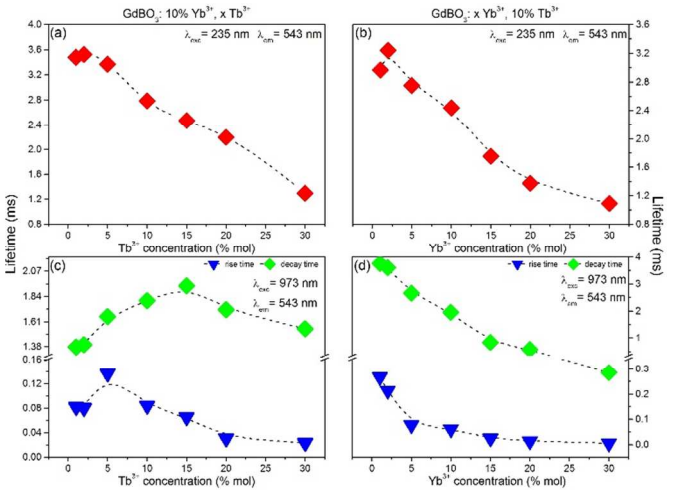

Fig. 7 Luminescence lifetimes (decays and rise times) of Tb^{3+} in $GdBO_3$ materials; dependence on the concentration of Tb^{3+} (a, c) and Yb^{3+} (b, d).

therefore energy transfer occurs faster. The longest rise times were calculated for samples doped with 5% of Tb^{3+} ions in the series of samples presented in Fig. 7c or 1% Yb^{3+} as showed in Fig. 7d.

The number of photons involved in the up-conversion process can be estimated from the dependence of integral luminescence intensity on pumping laser power at 973 nm. The relationship between up-conversion intensity I_{UC} and pumping laser intensity I_P is given by the following equation:

$$I_{UC} = \alpha(I_P)^n \quad (3)$$

where α is a proportionality factor and the exponent n represents the number of photons in the up-conversion process involved.[45] Fig. 8 presents the integral luminescence intensity plotted as a dependence on the energy of the pumping laser. The plotted points can be fit with a linear function which has a slope value of 2.45 ± 0.05. The obtained results suggest that at least two photons were involved in the energy transfer between Tb^{3+} and Yb^{3+} ions. The differences between the Tb^{3+} and Yb^{3+} energy levels enforce the cooperative energy transfer as the main mechanism responsible for the observed up-conversion.[19,46–48] In this process simultaneous interaction of two excited Yb^{3+} ions with one Tb^{3+} occurs, resulting in excitation of Tb^{3+} ions into the $^5D_4$ state. The observed higher than theoretical value of slope can be explained by the transfer of another photon between the Yb^{3+} and Tb^{3+} ion in the $^5D_4$ excited state, resulting in excitation to its $^5D_3$ state. Then the cross relaxation between Tb^{3+} populating $^5D_4$ from the $^5D_3$ excited state of the Tb^{3+} ion occurs, which is the most probable explanation for a higher number than 2 of photons involved in the observed UC and the lack of transitions from the $^5D_3$ excited state.

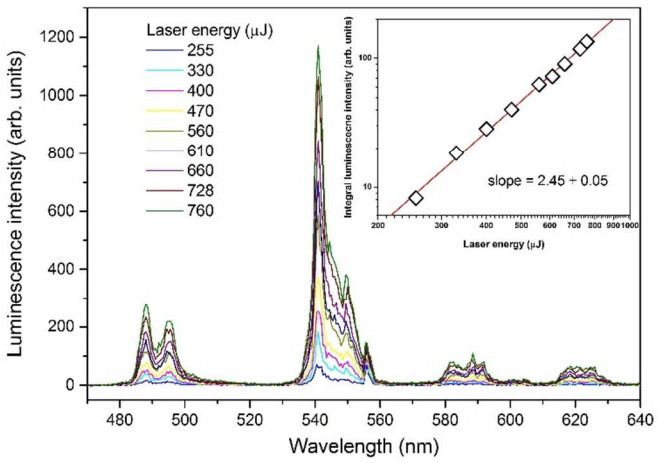

Fig. 8 Integral emission intensity of the $GdBO_3$:10%Yb^{3+},20%Tb^{3+} sample as a function of the pumping energy of the laser (λ_{ex} = 973 nm).

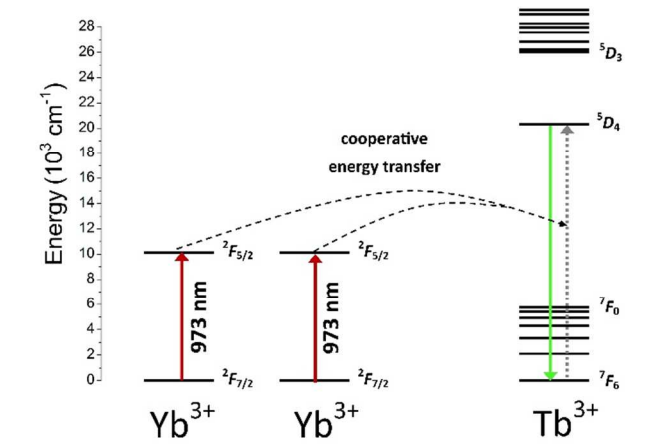

Fig. 9 Scheme of the energy transfer process responsible for the observed up-conversion occurring in the $GdBO_3$:Yb^{3+},Tb^{3+} samples.

The proposed mechanism of energy transfer between Yb^{3+} and Tb^{3+} ions leading to up-conversion luminescence is presented in Fig. 9. The excitation of Yb^{3+} ions under 973 nm wavelengths results in CET processes toward the excited state energy levels of the Tb^{3+} ions. The energy difference between the $^5D_4$ excited state of Tb^{3+} ions and the $^2F_{7/2}$ excited state of Yb^{3+} ions excludes sequential absorption of NIR photons. Therefore, one from the most often observed, energy transfer up-conversion process (ETU), can be excluded as responsible for the emission of our samples. This mechanism is typical for pairs of ions in which the sensitisers are Yb^{3+} ions and emitters are Er^{3+}, Tm^{3+} and Ho^{3+} ions.[9–11]

Conclusions

Gadolinium orthoborates doped by Yb^{3+} and Tb^{3+} ions can be synthesised by the sol-gel Pechini method followed by annealing of the precursors at 900 °C. XRD studies confirmed that the obtained materials were single phase and had a monoclinic crystal structure with the *C*2/*c* space group. As a result of Tb^{3+} and Yb^{3+} co-doping, the observed luminescence had a dual mode nature. The obtained materials could be excited by UV or NIR radiation, which resulted in intense green luminescence. Spectroscopic properties were analysed by collecting excitation and emission spectra under UV and NIR excitation. Luminescence decays were also measured. Excitation spectra in the UV range indicated that the $4f^8 \rightarrow 4f^7 5d^1$ transition of Tb^{3+} ions was strongly quenched by Yb^{3+} ions as a result of the charge transfer $Tb^{4+} \rightarrow Yb^{2+}$ state occurring in the samples. The highest luminescence under UV light (235 nm) excitation was observed in a sample doped only by 15% of Tb^{3+} ions. When NIR (973 nm) light was used, the highest emission was observed for a sample doped with 5% of Yb^{3+} and 20% of Tb^{3+} ions. Observed emission was based on transitions from the $^5D_4$ excited state of Tb^{3+} ions. Comparison between $GdBO_3$:5%Yb^{3+},20%Tb^{3+} sample and other Yb^{3+} and Tb^{3+} co-doped materials studied by our group clearly indicated that gadolinium borate is a better host compound presenting much more intense up-conversion luminescence (see Fig. 10). YPO_4, $LaPO_4$ and $GdPO_4$ doped by Yb^{3+} and Tb^{3+} ions were chosen as the best emitting from the series witch differed Yb^{3+} or Tb^{3+} concentrations.[14,15,49]

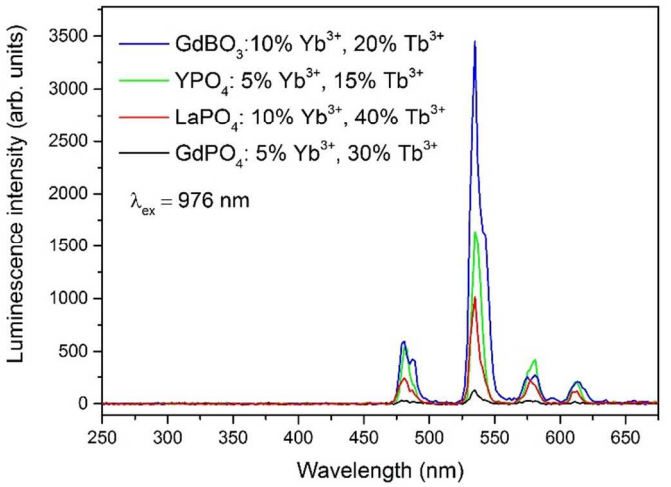

Fig. 10 Comparison of the up-conversion luminescence of materials doped by the optimal amount of Yb^{3+} and Tb^{3+} ions, giving the highest emission intensity.

By analysing the luminescence decays and calculated lifetime values we also found the effects of the presence of other quenching processes, such as cross relaxation between Tb^{3+} ions and backward energy transfer from Tb^{3+} to Yb^{3+} ions. The dependence of up-conversion luminescence intensity on pumping laser power affirmed that two photons took part in the excitation of Tb^{3+} ions.

Prepared materials can be applied in such areas as security markers or forensic sciences, where dual-mode luminescence is undoubtedly an advantage. The use of Yb^{3+}/Tb^{3+} based luminescence can improve currently used methods.

Acknowledgements

Funding for this research was provided by the National Science Centre (grant no. DEC-2011/03/D/ST5/05701).

Notes and references

Department of Rare Earth, Faculty of Chemistry, Adam Mickiewicz University, Umultowska 89b, 61-614 Poznan, Poland, e-mail: tgrzyb@amu.edu.pl

1 X. Li, S. Gai, C. Li, D. Wang, N. Niu, F. He, and P. Yang, *Inorg. Chem.*, 2012, **51**, 3963–71.
2 A. Gnach and A. Bednarkiewicz, *Nano Today*, 2012, **7**, 532–563.
3 M. Lin, Y. Zhao, S. Wang, M. Liu, Z. Duan, Y. Chen, F. Li, F. Xu, and T. Lu, *Biotechnol. Adv.*, 2012, **30**, 1551–61.
4 J.-C. G. Bünzli, *Acc. Chem. Res.*, 2006, **39**, 53–61.
5 A. Szczeszak, S. Lis, and V. Nagirnyi, *J. Rare Earths*, 2011, **29**, 1142–1146.
6 A. Szczeszak, T. Grzyb, S. Lis, and R. J. Wiglusz, *Dalt. Trans.*, 2012, **41**, 5824–31.
7 M. Wang, G. Abbineni, A. Clevenger, C. Mao, and S. Xu, *Nanomedicine Nanotechnology, Biol. Med.*, 2011, **7**, 710–729.
8 H. Li, J. Wang, F. Nan, S. Liang, Y. Zhong, L. Zhou, and Q. Wang, *Wuhan Univ. J. Nat. Sci.*, 2013, **18**, 207–212.
9 F. Auzel, *Chem. Rev.*, 2004, **104**, 139–73.
10 D. Vennerberg and Z. Lin, *Sci. Adv. Mater.*, 2011, **3**, 26–40.
11 M. Haase and H. Schäfer, *Angew. Chem. Int. Ed.*, 2011, **50**, 5808–29.
12 I. Hernández, N. Pathumakanthar, P. B. Wyatt, and W. P. Gillin, *Adv. Mater.*, 2010, **22**, 5356–60.
13 H. Wang, C. Duan, and P. A. Tanner, *J. Phys. Chem. C*, 2008, **112**, 16651–16654.
14 T. Grzyb, A. Gruszeczka, R. J. Wiglusz, and S. Lis, *J. Mater. Chem. C*, 2013, **1**, 5410–5418.
15 T. Grzyb, A. Gruszeczka, R. J. Wiglusz, Z. Śniadecki, B. Idzikowski, and S. Lis, *J. Mater. Chem.*, 2012, **22**, 22989–22997.
16 P. Li, Q. Peng and Y. Li, *Adv. Mater.*, 2009, **21**, 1945–1948.
17 P. Kumar, J. Dwivedi and B. K. Gupta, *J. Mater. Chem. C*, 2014, **2**, 10468–10475.
18 C. H. Yang, Y. X. Pan, Q. Y. Zhang, and Z. H. Jiang, *J. Fluoresc.*, 2007, **17**, 500–504.
19 G. M. Salley, R. Valiente, and H. U. Guedel, *J. Lumin.*, 2001, **94-95**, 305–309.
20 H. Moos, *J. Lumin.*, 1970, **1-2**, 106–121.
21 K. Nakamoto, *Infrared and Raman Spectra of Inorganic and Coordination Compounds Part A: Theory and Applications in Inorganic Chemistry*, Wiley 2009.
22 Y. Arai, T. Yamashidta, T. Suzuki, and Y. Ohishi, *J. Appl. Phys.*, 2009, **105**, 83105–83111.
23 E. M. Levin, R. S. Roth, and J. B. Martin, *Am. Miner.*, 1961, **20**, 283–287.
24 M. Ren, J. H. Lin, Y. Dong, L. Q. Yang, M. Z. Su, and L. P. You, *Chem. Mater.*, 1999, **11**, 1576–1580.
25 G. Chadeyron, M. El-Ghozzi, R. Mahiou, A. Arbus, and J. Cousseins, *J. Solid State Chem.*, 1997, **128**, 261–266.
26 R. E. Newnham, M. J. Redman and R. P. Santoro, *J. Am. Ceram. Soc.*, 1963, **46**, 253–256.
27 W. F. Bradley, D. L. Graf, and R. S. Roth, *Acta Crystallogr.*, 1966, **20**, 283–287.
28 J. Holsa, *Inorg. Chim. Acta*, 1987, **139**, 257–259.
29 J. Lin, D. Sheptyakov, Y. Wang, and P. Allenspach, *Chem. Mater.*, 2004, **16**, 2418–2424.
30 P. E. D. Morgan, P. J. Carroll, and F. F. Lange, *Mater. Res. Bull.*, 1977, **12**, 251–259.
31 G. Jia, P. A. Tanner, C.-K. Duan, and J. Dexpert-Ghys, *J. Phys. Chem. C*, 2010, **114**, 2769–2775.
32 A. Pitscheider, R. Kaindl, O. Oeckler, and H. Huppertz, *J. Solid State Chem.*, 2011, **184**, 149–153.
33 A. Szczeszak, T. Grzyb, B. Barszcz, V. Nagirnyi, A. Kotlov, and S. Lis, *Inorg. Chem.*, 2013, **52**, 4934–4940.
34 A. Szczeszak, T. Grzyb, S. Lis, and R. J. Wiglusz, *Dalt. Trans.*, 2012, **41**, 5824–5831.
35 L. Ning, C. Mak, and P. Tanner, *Phys. Rev. B*, 2005, **72**, 085127.
36 L. Yang, L. Zhou, X. Chen, X. Liu, P. Hua, Y. Shi, X. Yue, Z. Tang, and Y. Huang, *J. Alloy. Compd.*, 2010, **509**, 3866–3871.
37 J.-L. Yuan, X.-Y. Zeng, J.-T. Zhao, Z.-J. Zhang, H.-H. Chen, and X.-X. Yang, *J. Phys. D Appl. Phys.*, 2008, **41**, 105406.
38 X. Liu, S. Ye, Y. Qiao, G. Dong, B. Zhu, D. Chen, G. Lakshminarayana, and J. Qiu, *Appl. Phys. B*, 2009, **96**, 51–55.
39 Q. Y. Zhang, C. H. Yang, Z. H. Jiang, and X. H. Ji, *Appl. Phys. Lett.*, 2007, **90**, 061914.
40 P. Berdowski, M. J. J. Lammers, and G. Blasse, *Chem. Phys. Lett.*, 1985, **113**, 387–390.
41 P. C. Ricci, M. Salis, R. Corpino, C. M. Carbonaro, E. Fortin, and A. Anedda, *J. Appl. Phys.*, 2010, **108**, 43512–43517.
42 A. D. Sontakke, K. Biswas, and K. Annapurna, *J. Lumin.*, 2009, **129**, 1347–1355.
43 T. Yamashita and Y. Ohishi, *J. Non-Cryst. Solids*, 2008, **354**, 1883–1890.
44 T. Grzyb, M. Runowski, A. Szczeszak, and S. Lis, *J. Phys. Chem. C*, 2012, **116**, 17188–17196.
45 R. Scheps, *Ptog. Quant. Electron.*, 1996, **20**, 271–358.
46 G. Salley, R. Valiente, and H. Güdel, *Phys. Rev. B*, 2003, **67**, 1–9.
47 I. a. a. Terra, L. J. Borrero-González, L. a. O. Nunes, M. P. Belançon, J. H. Rohling, M. L. Baesso, and O. L. Malta, *J. Appl. Phys.*, 2011, **110**, 083108.
48 W. Stręk, A. Bednarkiewicz, and P. J. Dereń, *J. Lumin.*, 2001, **92**, 229–235.
49 T. Grzyb, R.J. Wiglusz, A. Gruszeczka, S. Lis, *Dalton Trans.*, 2014, **43**, 17255–17264.

Table of contents

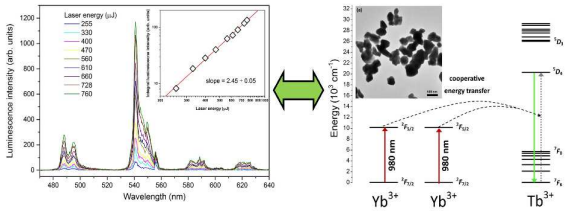

Gadolinium orthoborates doped with Yb^{3+} and Tb^{3+} ions, showing dual-mode luminescence (down- and up-conversion) were synthesised by the sol-gel Pechini method and analysed.